

Dysmyelination not demyelination causes neurological symptoms in preweaned mice in a murine model of Cockayne syndrome

Ingrid Revet^a, Luzviminda Feeney^a, Amy A. Tang^b, Eric J. Huang^b, and James E. Cleaver^{a,1}

Departments of ^aDermatology and ^bPathology, University of California, San Francisco, CA 94143

Contributed by James E. Cleaver, February 15, 2012 (sent for review October 21, 2011)

Cockayne syndrome (CS) is a rare autosomal recessive neurodegenerative disease that is associated with mutations in either of two transcription-coupled DNA repair genes, *CSA* or *CSB*. Mice with a targeted mutation in the *Csb* gene (*Cs-b^{m/m}*) exhibit a milder phenotype compared with human patients with mutations in the orthologous *CSB* gene. Mice mutated in *Csb* were crossed with mice lacking *Xpc* (*Xp-c^{-/-}*), the global genome repair gene, to enhance the pathological symptoms. These *Cs-b^{m/m}.Xp-c^{-/-}* mice were normal at birth but exhibited progressive failure to thrive, whole-body wasting, and ataxia and died at approximately postnatal day 21. Characterization of *Cs-b^{m/m}.Xp-c^{-/-}* brains at postnatal stages demonstrated widespread reduction of myelin basic protein (MBP) and myelin in the sensorimotor cortex, the stratum radiatum, the corpus callosum, and the anterior commissure. Quantification of individual axons by electron microscopy showed a reduction in both the number of myelinated axons and the average diameter of myelin surrounding the axons. There were no significant differences in proliferation or oligodendrocyte differentiation between *Cs-b^{m/m}.Xp-c^{-/-}* and *Cs-b^{m/+}.Xp-c^{-/-}* mice. Rather, *Cs-b^{m/m}.Xp-c^{-/-}* oligodendrocytes were unable to generate sufficient MBP or to maintain the proper myelination during early development. *Csb* is a multifunctional protein regulating both repair and the transcriptional response to reactive oxygen through its interaction with histone acetylase p300 and the hypoxia-inducible factor (HIF)1 pathway. On the basis of our results, combined with that of others, we suggest that in *Csb* the transcriptional response predominates during early development, whereas a neurodegenerative response associated with repair deficits predominates in later life.

transcription-coupled repair | behavior | rotenone | γ H2AX

Cockayne syndrome (CS) is a rare autosomal recessive neurodegenerative disease, with a wide range of severity, including cachectic dwarfism, retinopathy, optic nerve atrophy, microcephaly, deafness with cochlea loss, neural defects, ganglial calcification, and retardation of growth and development after birth; patients with CS have a lifespan that varies widely, with an average of 12.5 y (1–3). In humans and mice the cerebellum shows distinctive atrophy with loss of Purkinje cells that are associated with regulating balance and walking (4, 5). The brains of CS patients and mice have shown evidence for accumulation of unrepaired damage (6, 7). The brain shows reduced numbers of oligodendrocytes and less myelination, but it remains unclear whether the disease is primarily one of neurodegeneration with neuronal and myelin loss (demyelination) or a failure of oligodendrocyte differentiation and myelin synthesis (dysmyelination) (4).

DNA nucleotide excision repair (NER) has two main branches: global genome repair (GGR), which is associated with repair of nontranscribed regions of the genome; and transcription-coupled repair (TCR), which is associated with enhanced repair of the transcribed strand of active genes. CS is associated with mutations in two genes dedicated to TCR, *CSA* and *CSB*. These are cofactors for RNA polymerase II that facilitate increased rates of repair of the transcribed strand and continuous transcription through sites of DNA damage (3, 8). Evidence from the analogous system

in *Escherichia coli*, the *mfd* protein, suggests that one function is to displace the transcription apparatus during head-on collisions between replication and transcription (9). Consequently, CS cells show reduced recovery of RNA and DNA synthesis after UV damage (10). Patients have also been reported with mild photosensitivity and no reported neurological symptoms, named UV^s (11, 12), and with a very severe disorder known as cerebro-oculo-facio-skeletal syndrome (COFS) (13). These extremes of CS are associated with mutations in *CSA*, *CSB*, and at least one other presently uncharacterized gene but have similar cellular defects in UV sensitivity and TCR to other CS patients (14–17).

Despite extensive knowledge about the molecular functions of the *CSA* and *CSB* proteins and their role in TCR and chromatin remodeling (3, 8, 18–21), the mechanisms by which these proteins are involved in neuropathology is still largely speculative. Suggestions have been made that CS caused by faulty responses to endogenously generated oxidative damage through additional deficiencies in base excision repair (18), mitochondrial activity (22), and coordination of a transcriptional response (4, 23). However, although *CSA* and *CSB* patients have indistinguishable clinical disease, only *CSB* and not *CSA* or UV^s cells are sensitive to oxidative damage (14, 17, 24).

We have analyzed a mouse model of CS in which both TCR (*Csb*) and GGR (*Xpc*) were removed by gene targeting (the *Cs-b^{m/m}.Xp-c^{-/-}* mouse strain). The *Csb* mutation (*Cs-b^{m/m}*) mimics a truncation found in a human CS patient. Neither human nor mouse mutated in *XPC* show any neuropathology (3). Previously, we demonstrated that major neurological deficiencies occurred in the cerebellum, with the granule cells demonstrating high TUNEL staining indicative of apoptosis (25). Purkinje cells, identified by the marker calbindin, were severely depleted and, although not TUNEL-positive, displayed strong immunoreactivity for p53, indicating cellular stress.

Here, we report that the neural phenotype in *Cs-b^{m/m}.Xp-c^{-/-}* mice is attributable primarily to widespread dysmyelination resulting from the inability of oligodendrocytes to produce or maintain normal levels of myelination after terminal differentiation. This observation contrasts with the idea that premature re-entry of differentiated neural cells into cycle could trigger apoptosis (26). Our results also indicate that not all of the symptoms of NER diseases necessarily represent premature aging and degenerative disorders (5, 27). Because *Csb* is a multifunctional protein regulating both repair and the transcriptional response to reactive oxygen species (ROS) (4, 28) we suggest that defective transcriptional regulation may predominate during early development to generate the dysmyelination phenotype, whereas

Author contributions: I.R., L.F., A.A.T., E.J.H., and J.E.C. designed research; I.R., L.F., A.A.T., E.J.H., and J.E.C. performed research; A.A.T. and E.J.H. contributed new reagents/analytic tools; I.R., E.J.H., and J.E.C. analyzed data; and I.R., E.J.H., and J.E.C. wrote the paper.

The authors declare no conflict of interest.

¹To whom correspondence should be addressed. E-mail: jcleaver@cc.ucsf.edu.

This article contains supporting information online at www.pnas.org/lookup/suppl/doi:10.1073/pnas.1202621109/-DCSupplemental.

repair deficiencies resulting in a neurodegenerative disorder may predominate in later life.

Results

Body Weight, Brain Weight, and Survival. The $Csb^{m/m}.Xpc^{-/-}$ mice were normal at birth but failed to thrive and steadily lagged behind their littermates in both body weight and brain weight (Fig. S1) and exhibited whole-body wasting and ataxia and died around postnatal day (P)21, with an ~50% reduction in body weight (25). Heterozygosity in the *Csb* gene on the $Xpc^{-/-}$ background produced a viable strain with no apparent neurological symptoms (Fig. S1). A similar but more severe phenotype has been reported in the double mutant strain $Csb^{m/m}.Xpa^{-/-}$ (29). In our studies, we compared strains homozygous and heterozygous for *Csb*, on the *Xpc*-negative background, to identify those features of the pathology dictated by complete loss of *Csb* functions. The *Xpc* strain exhibits no reported neurological dysfunction but, like XP-C patients, develops skin cancer after exposure to UV light (30). The mild phenotype of the $Csb^{m/m}$ strain alone and the very severe phenotype of the double mutant are reminiscent of the human extremes of CS symptoms that present as the UV^s and the COFS disorders.

Behavioral Deficits in Double Mutant Mice. The abnormal clasp reflex and complete inactivity upon tail suspension observed in the double mutant (Fig. 1A) is typical of mouse models of neurodegeneration (31). Similarly, in a rotarod test, the double mutant mice were unable to stay on the rotating beam (Fig. 1B), whereas the strain heterozygous for *Csb* held for extended periods, similar to those seen in completely wild-type mice. The double mutant mice also showed deficits in the catwalk gait analysis test (Fig. 1C). Similar behavior is observed in other DNA repair-deficient mouse models (32, 33). These behaviors correspond to human patients who show difficulty walking and eventually become wheel chair bound (1).

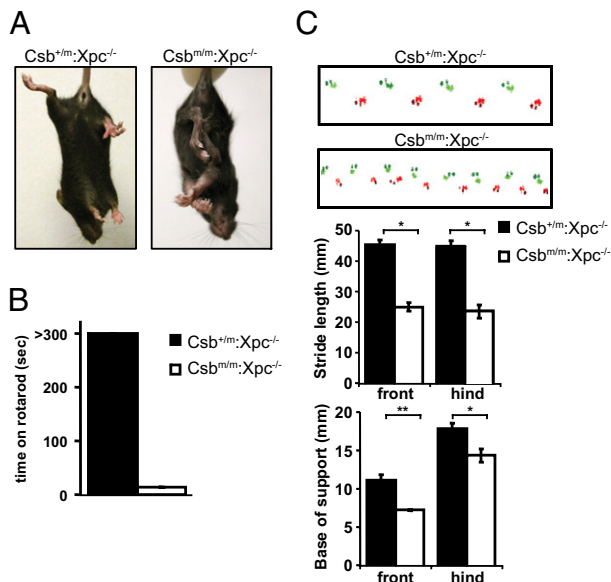


Fig. 1. Neurological defects in P17 $Csb^{m/m}.Xpc^{-/-}$ mice compared with $Csb^{+/m}.Xpc^{-/-}$ littermates. (A) Limb-clasping reflex in mice suspended by the tail. (B) Rotarod analysis measures the ability to run on a rotating cylinder. Any mouse that stayed on the rod for the full 30 s was allocated a maximum value of 300. (C) Catwalk analysis. Light green depicts the right front paws, dark green the right hind paws, light red the left front paws, and dark red the left hind paws. Stride length and base of support measured in millimeters for front and hind paws. Each assay point represents at least five mice. A significant difference was found according to Student *t* test (* $P = 0.02$; ** $P = 0.04$).

General Brain Architecture: Normal Except for Loss of MBP. We previously reported that the $Csb^{m/m}.Xpc^{-/-}$ mice showed extensive cerebellar pathology and loss of Purkinje cells, similar to human patients (1, 5, 34). The general architecture of the brain stained by hematoxylin/eosin (H&E), NeuN, and glial fibrillary acidic protein (GFAP) appeared normal at p7 and p17 (p17 only shown in Fig. S2). In the cerebral cortex, anterior commissure, corpus callosum, and dentate gyrus, however, we observed a decrease in the myelin basic protein (MBP) in $Csb^{m/m}.Xpc^{-/-}$ mice compared with *Csb* heterozygotes ($Csb^{+/m}.Xpc^{-/-}$) (Fig. 2A and B and Fig. S2). Most notably, the sagittal sections show a clear reduction in the number of axons stained with MBP in the hippocampus and anterior commissure of $Csb^{m/m}.Xpc^{-/-}$ mice at p13 (Fig. 2A and B).

MBP Axon Numbers and Thickness. To determine whether the reduced MBP staining (Fig. S2) translated in a compromised myelin density, we analyzed sagittal sections of the anterior commissure by electron microscopy. This showed a severe reduction in the numbers of axons in both the anterior commissure and the corpus callosum (Fig. S3), and the membranes of individual axons were hypomyelinated (Fig. 2C–E).

Oligodendrocyte Maturation: Double Labeling with Olig2 and BrdU. The severe reduction in MBP and axon numbers suggests that the oligodendrocytes may be unable to differentiate and become mature MBP-synthesizing cells. We tested this possibility by labeling the mice with BrdU to identify proliferating cells and killed mice at P7 and P18 and stained with olig2 and BrdU antibodies (Fig. 3). There was, however, no significant difference between heterozygous and homozygous mice either at P7 or P18. Both genotypes showed a similar reduction in oligodendrocyte numbers and reduction of BrdU labeling of oligodendrocytes, which suggests that oligodendrocytes differentiate and exit the cell cycle normally but do not mature into MBP-synthesizing cells. The subsequent deficits in MBP are then sufficient to cause neuronal dysfunction with pathological and behavioral consequences. This phenotype is more clearly related to dysmyelination than to a degradation of preexisting myelin. The failure of differentiated cells to synthesize large quantities of specific gene product is reminiscent of the phenotype of trichothiodystrophy (TTD) in which mutations in *XPD*, part of the TFIIH transcription factor, result in terminally differentiated cells being unable to synthesize myelin, keratin and other specific products (35–37). Because the *CSB* gene is a cofactor to RNA Pol II, we speculate that high levels of transcription necessary for the production of MBP cannot be generated in the double mutant.

Histone Deacetylase p300 in the Response to DNA Damage. *Csb* plays a role in the responses to endogenously generated oxidative damage through additional deficiencies in base excision repair (18), mitochondrial activity (22), and coordination of a transcriptional response (4, 23). As part of the transcription response, *Csb* displaces the histone acetylase p300 from p53, resulting in activation of the hypoxic hypoxia-inducible factor (HIF)1 α response (23). We, therefore, questioned whether abrogation of p300 itself would affect either the UV or the ROS response. Mouse knockouts of p300 are not viable, and their fibroblasts senesce prematurely, and only SV40-transformed mouse embryo fibroblasts are available (38). $Csb^{m/m}$ cells were sensitive to both rotenone and UV damage (Fig. 4A and B). $p300^{-/-}$ cells, however, were more sensitive than wild-type cells to killing by endogenous ROS generated by rotenone (Fig. 4D) (39, 40) but were not UV-sensitive (Fig. 4C). The DNA damage marker γ H2Ax only showed an increase following UV exposure, not rotenone (Fig. 4E), suggesting limited DNA damage from endogenous ROS. These observations suggest that loss of *Csb* can cause UV sensitivity through its role as a cofactor for RNA Pol II and TCR, and independently cause

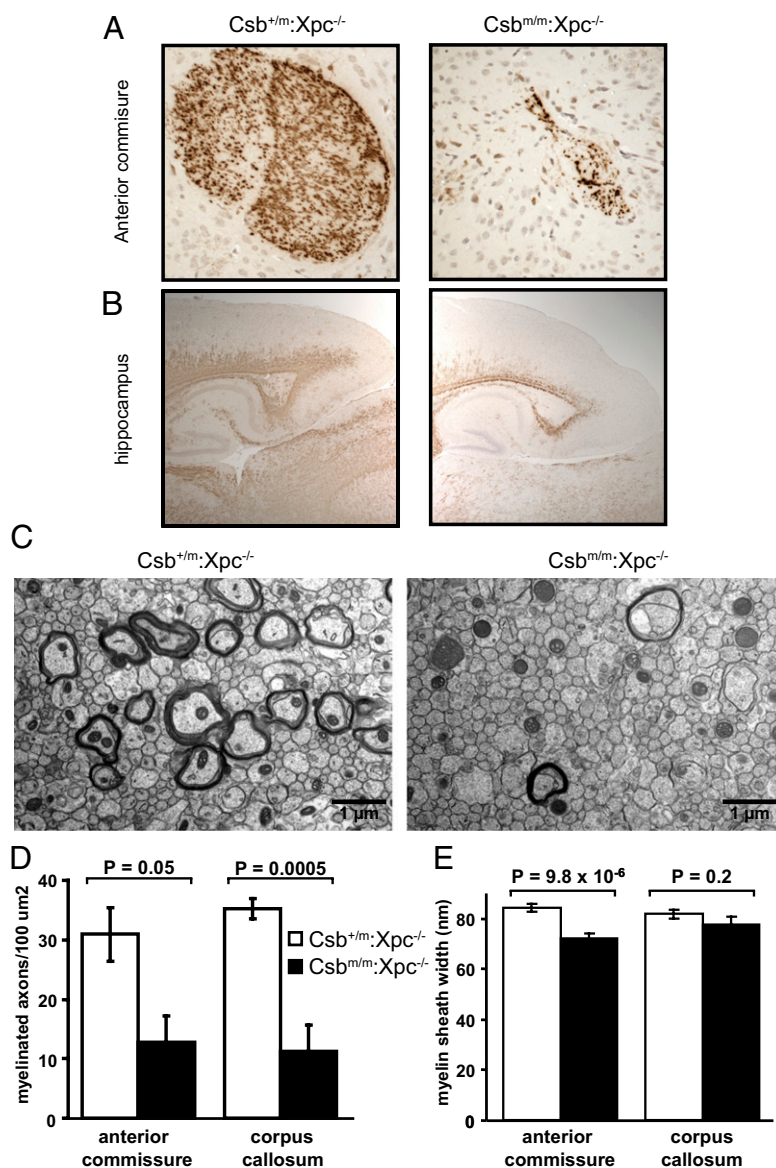


Fig. 2. Hypomyelination in $\text{Cs-b}^{m/m}.\text{Xp-c}^{-/-}$ mice. Sagittal brain sections of P13 $\text{Cs-b}^{m/m}.\text{Xp-c}^{-/-}$ and $\text{Cs-b}^{+/m}.\text{Xp-c}^{-/-}$ depicting the anterior commissure (A) and hippocampus (B) stained with MBP showing a reduction in $\text{Cs-b}^{m/m}.\text{Xp-c}^{-/-}$ mice. (C) Electron micrographs of the anterior commissure of P17 $\text{Cs-b}^{m/m}.\text{Xp-c}^{-/-}$ deficient mice compared with $\text{Cs-b}^{+/m}.\text{Xp-c}^{-/-}$ littermates. (D and E) Number of myelinated axons per $100 \mu\text{m}^2$ (D) and myelin sheath width in, respectively, anterior commissure and corpus callosum of $\text{Cs-b}^{m/m}.\text{Xp-c}^{-/-}$ mice compared with $\text{Cs-b}^{+/m}.\text{Xp-c}^{-/-}$ (E).

sensitivity to ROS, although loss of transcriptional regulation, via p300 interaction. The failure of differentiated oligodendrocytes to synthesize MBP could then be attributable to the deficiency in transcriptional response to endogenous ROS and not because of a deficient repair of DNA lesions by TCR (4, 37).

Discussion

There remains a major challenge in relating the wide range of functions of the CSB protein to the similarly wide range of clinical symptoms in human and mouse (18, 41). The CSB protein has been reported to be involved in the TCR of large DNA adducts, base excision repair, recovery of RNA synthesis as a cofactor of RNA pol II, chromatin remodeling, the transcriptional response to ROS, and, most recently, in mitochondrial function (3, 4, 8, 18–22, 28, 37). Humans and mice show growth failure, pathological aging, hypomyelination, and neurodegeneration (1, 2, 42). No correlation has yet been made between sites of mutation in the

CSB gene and the severity of clinical symptoms (18, 41); patients with no detectable CSB protein may be affected either severely (13, 43, 44) or mildly (45). Most relevant to our study, patients show reduced cerebellar function with hypomyelination and white matter loss (1). Mutant mice show similar features, although with lower penetrance in single $\text{Csb}^{m/m}$ mutants. Double mutant mice, either $\text{Cs-b}^{m/m}.\text{Xp-a}^{-/-}$ or, as described here, the $\text{Cs-b}^{m/m}.\text{Xp-c}^{-/-}$ strain, have reduced body weight and progressive cachexia, photoreceptor loss, cochlea hair cell loss, and motor dysfunction and are sensitive to ionizing radiation and oxidative damage (2, 42).

Our gross functional analysis recapitulates features already described in $\text{Cs-b}^{m/m}.\text{Xp-c}^{-/-}$ mice (5), but we have now concentrated on the hypomyelination distinctive for human patients, especially COFS patients, who have a similar extremely shortened lifespan to these mice (13). The preweaning period is one of cell proliferation and differentiation in the brain, leading to the development of MBP, which coats developing neurons. We observed a striking

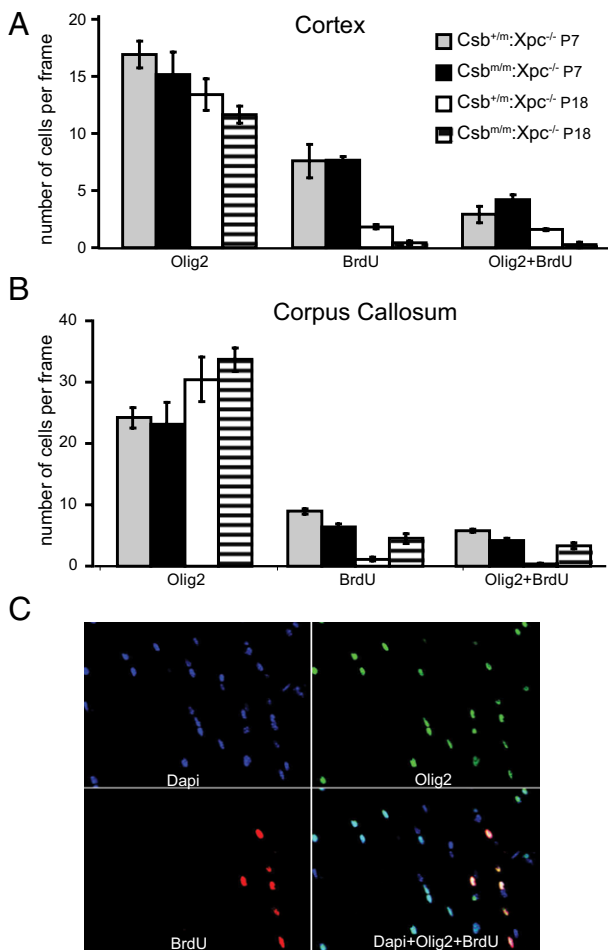


Fig. 3. (A and B) BrdU and Olig2 staining of P7 and P18 Cs-b^{m/m}.Xp-c^{-/-} mice compared with Cs-b^{m/m}.Xp-c^{-/-} littermates in the cortex (A) or corpus callosum (B). (C) Corpus callosum staining of P7 Cs-b^{m/m}.Xp-c^{-/-} mice with, respectively, DAPI in blue, olig2 in green, and BrdU in red.

reduction in the synthesis of MBP and corresponding reduction in the numbers of axons and their membrane thickness. This was particularly evident in the cortex and by the atrophy of the anterior commissure. Previous analysis of human CS-B and mouse Cs-b concentrated on the Purkinje layer in the cerebellum that appears to be a major site of degeneration (5, 46). This layer has elevated p53 and shows accumulation of the DNA damage markers ATM and Mre11 (5, 46). We previously reported increased expression of MBP in the cerebellum of Cs-b^{-/-} mice (5), as also reported for Ttd^{-/-} mice that correspond to the human disorder TTD (37), showing that there is considerable regional variation in MBP expression. Our study now shows that hypomyelination is widespread in the brain, consistent with human symptomatology, and was not associated with visible degenerative pathology. Myelination is required for efficient propagation of action potentials in neurons, so the abnormal myelination pattern in the Cs-b;Xp-c double mutants may result in defective functions in the generation, propagation, and maintenance of their action potentials. Defective action potentials would contribute to the behavioral, motor, and cognitive impairments of CS patients.

Our results allow us to consider possible mechanisms for hypomyelination. Two major interpretations of the NER disorders attribute the symptoms either to a DNA repair disorder or to a defective transcriptional response (4). In both interpretations, the ultimate cause may be endogenous ROS, but only the DNA repair hypothesis requires actual DNA damage. TTD is a disorder

of DNA repair associated with mutations in components of the transcription factor TFIIH, which promotes the recruitment of thyroid hormone and vitamin D receptors to promoters involved in myelination, acting as a coactivator for MBP synthesis (37). CS, however, does not show abnormalities in nuclear hormone and vitamin D receptors, indicating that CS involves a different mechanism of dysmyelination to Ttd (47). In contrast, in conditional mutants of Cs-b^{m/m}.Xp-a^{-/-} mice, elimination of GGR late in life sets up a demyelination phenotype (48), suggesting that dysmyelination predominates during early development associated with TCR defects, whereas a neurodegenerative response associated with GGR deficits predominates in later life.

Our results in p300 knockout cells suggests that loss of the HIF1 α response pathway that regulates the response to reactive ROS can have significant effects on the response to endogenous damage but not UV. Alternatively, less specific mechanisms such as chronic inflammatory stress and microvasculature may be involved (4, 49). The arrest of transcription in CS cells is a strong apoptotic signal (50, 51), and we previously observed apoptotic cells in the cerebellum of Cs-b^{m/m}.Xp-c^{-/-} mice (5). In the present study we did not observe widespread apoptosis, but observed an orderly reduction in BrdU labeled oligodendrocytes in cortex and anterior commissure of heterozygous and homozygous Cs-b^{m/m} mice. Apparently, the differentiated oligodendrocytes are unable to support synthesis of major terminal products such as MBP, analogous to the situation observed in TTD. This failure may be due to accumulated ROS damage, and the loss of the Csb/p300 interaction that regulates the response to ROS (23).

CS, therefore, represents a developmental disorder of dysmyelination that is especially distinct in COFS, the severest form of CS with a very short lifespan similar to our double mutant mice (13). This pathology differs from chronic neurodegenerative diseases that exhibit demyelination, such as multiple sclerosis, or neuronal cell death attributable to protein aggregation such as Parkinson disease, Huntington disease, and amyotrophic lateral sclerosis. Therapeutic intervention may, therefore, require attention to the sources of endogenous DNA damage and mechanisms of remyelination that could by-pass the DNA repair defect.

Materials and Methods

Mouse Breeding. A parental Cs-b^{m/m}.Xp-c^{-/-} strain was established (5) from Cs-b^{m/m} mice [a gift from G. T. van der Horst and J. H. Hoeymakers, Erasmus University Medical Center, Rotterdam, The Netherlands (52)] and Xp-c^{-/-} mice [purchased from Taconic (53)]. Genotypes were monitored by PCR (see *SI Materials and Methods*). When the parental strain was bred, we obtained three genotypes in Mendelian ratios, but the double homozygote failed to thrive and died before weaning at 14–21 d. Studies of the homozygote were, therefore, confined to the period up to 17 d. Behavioral analysis was performed at the University of California San Francisco (UCSF) Neurobehavioral Core for Rehabilitation Research (NCRR) using three main tests: clasping reflex, rotarod test, and catwalk (see *SI Materials and Methods*). All data were assembled from five or more mice per genotype and expressed as SEMs.

Histological Analysis. Mice were killed with an overdose of anesthetic (2,2,2-tribromoethanol) and perfused transcardially with PBS followed by the 4% paraformaldehyde fixative. For BrdU staining, mice were injected i.p. with BrdU (Roche Applied Science) dissolved in PBS (50 mg/kg) 24 h before they were killed. Brains were removed, postfixed in the same fixative overnight at 4 °C, and paraffin-embedded. Tissue was sectioned at 5- μ m thickness sagittally or coronally and placed on precoated slides. The following primary antibodies were used for immunohistochemistry: NeuN (MAB377; Millipore), GFAP (3670; Cell Signaling), and MBP (Sc-13914; Santa Cruz Biotechnology). The olig2 antibody was kindly provided by David Rowitch (Department of Pediatrics and Howard Hughes Institute, University of California, San Francisco, CA). Immunocomplexes were visualized using appropriate, Alexa 488- or 568-conjugated (Invitrogen) or biotinylated (Vector Labs) secondary antibodies followed by mounting in Vectashield with DAPI (H-1200; Vector Labs) or staining with a Vectastain kit (PK-6100; Vector Labs), respectively, according to the protocol of the manufacturer.

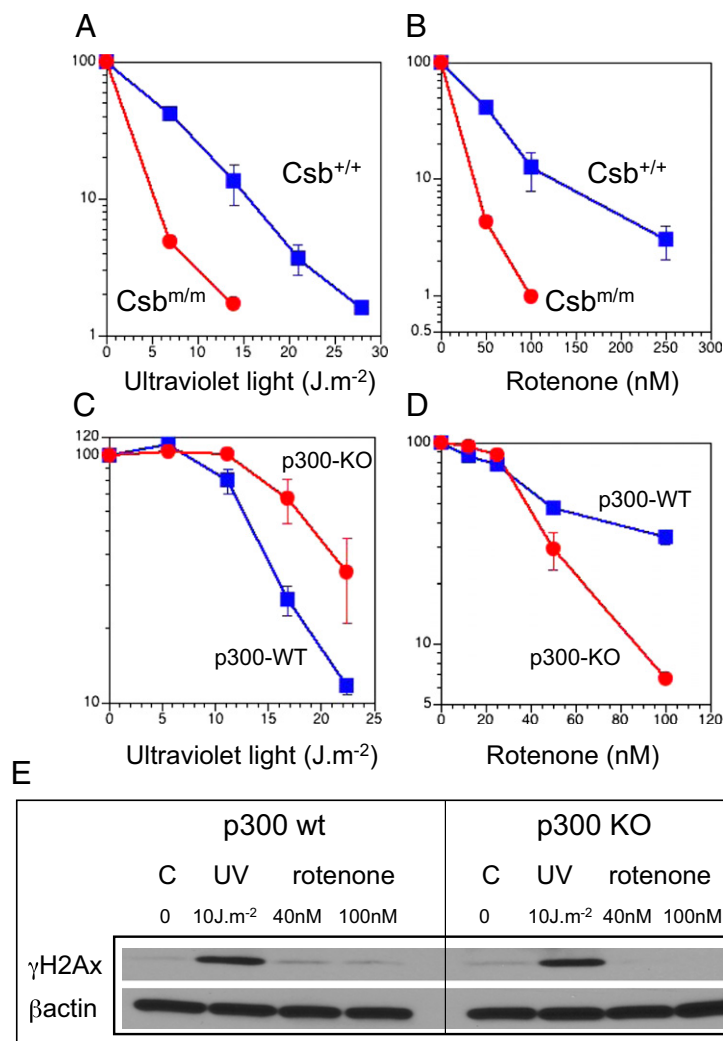


Fig. 4. DNA damage response in *Csb^{tm/m}*, p300 knockout, and wild-type mouse embryonic fibroblasts. (A) Survival of *Csb^{tm/m}* (red circles) and wild-type (blue squares) cells to UV light. (B) Survival of *Csb^{tm/m}* (red circles) and wild-type (blue squares) cells to ROS generated from continuous exposure to rotenone. (C) Survival of p300 knockout (red circles) and wild-type (blue squares) cells to UV light. (D) Survival of p300 knockout (red circles) and wild-type (blue squares) cells to ROS from continuous exposure to rotenone. (E) Induction of γ H2Ax 4 h after UV irradiation or the start of exposure to rotenone in p300 knockout and wild-type cells. Note low level of γ H2Ax in wild-type cells and complete absence from knockout cells. Error bars represent SD of six determinations.

Electron Microscopy. For electron microscopy, mice were killed with an overdose of anesthetic (Avertin) and perfused transcardially with PBS, followed by the 4% paraformaldehyde fixative. Brains were removed and postfixed in the same fixative overnight at 4 °C. For electron microscopy, the blocs of tissue were dehydrated with a graded series of ethanol solutions, cleared with propylene oxide, and embedded in polymerized Eponate 12 (Ted Pella). Ultrathin sections (1 μ m) were cut with a microtome (Reichert-Jung) and collected on copper grids. Sections were examined with a JEOL 1200EX electron microscope.

Tissue Culture. Mouse embryonic fibroblasts (MEFs), *Cs-b^{tm/m}* and wild-type, were developed from embryos by standard techniques (donated by W. Bohr,

National Institutes on Aging, Baltimore, MD). p300 knockout and wild-type SV40-transformed MEFs were donated by J. A. DeCaprio (Dana Farber Institute, Boston, MA) (38).

ACKNOWLEDGMENTS. We thank Linda Noble and Sandra Canchola from the UCSF NCRF for their expertise and help with the neurobehavioral analysis. This work was supported by National Institute of Neurological Disorders and Stroke Grant 5R01NS052781, the University of California Cancer Research Coordinating Committee, the UCSF Edward Dickson Emeritus Professorship (J.E.C.), and generous donations from The Luke O'Brien Foundation, the Xeroderma Pigmentosum Family Support Group, and The Taube Neurological Fund, Osher Center, San Francisco.

- Nance MA, Berry SA (1992) Cockayne syndrome: Review of 140 cases. *Am J Med Genet* 42:68–84.
- Weidenheim KM, Dickson DW, Rapin I (2009) Neuropathology of Cockayne syndrome: Evidence for impaired development, premature aging, and neurodegeneration. *Mech Ageing Dev* 130:619–636.
- Cleaver JE, Lam ET, Revet I (2009) Disorders of nucleotide excision repair: The genetic and molecular basis of heterogeneity. *Nat Rev Genet* 10:756–768.
- Brooks PJ, Cheng T-F, Cooper L (2008) Do all of the neurologic diseases in patients with DNA repair gene mutations result from the accumulation of DNA damage? *DNA Repair (Amst)* 7:834–848.
- Laposa RR, Huang EJ, Cleaver JE (2007) Increased apoptosis, p53 up-regulation, and cerebellar neuronal degeneration in repair-deficient Cockayne syndrome mice. *Proc Natl Acad Sci USA* 104:1389–1394.
- Hayashi M, Araki S, Kohyama J, Shioda K, Fukatsu R (2005) Oxidative nucleotide damage and superoxide dismutase expression in the brains of xeroderma pigmentosum group A and Cockayne syndrome. *Brain Dev* 27:34–38.
- Kirkali G, de Souza-Pinto NC, Jaruga P, Bohr VA, Dizdaroglu M (2009) Accumulation of (5'S)-8,5'-cyclo-2'-deoxyadenosine in organs of Cockayne syndrome complementation group B gene knockout mice. *DNA Repair (Amst)* 8: 274–278.

8. Hoeijmakers JH (2001) Genome maintenance mechanisms for preventing cancer. *Nature* 411:366–374.
9. Pomerantz RT, O'Donnell M (2010) Direct restart of a replication fork stalled by a head-on RNA polymerase. *Science* 327:590–592.
10. Lehmann AR, Kirk-Bell S, Mayne L (1979) Abnormal kinetics of DNA synthesis in ultraviolet light-irradiated cells from patients with Cockayne's syndrome. *Cancer Res* 39:4237–4241.
11. Fujiwara Y, Ichihashi M, Kano Y, Goto K, Shimizu K (1981) A new human photosensitive subject with a defect in the recovery of DNA synthesis after ultraviolet-light irradiation. *J Invest Dermatol* 77:256–263.
12. Itoh T, Fujiwara Y, Ono T, Yamaizumi M (1995) UVs syndrome, a new general category of photosensitive disorder with defective DNA repair, is distinct from xeroderma pigmentosum variant and rodent complementation group I. *Am J Hum Genet* 56:1267–1276.
13. Laugel V, et al. (2008) CofS syndrome: Three additional cases with CSB mutations, new diagnostic criteria and an approach to investigation. *J Med Genet* 45:564–571.
14. Spivak G, Hanawalt PC (2006) Host cell reactivation of plasmids containing oxidative DNA lesions is defective in Cockayne syndrome but normal in UV-sensitive syndrome fibroblasts. *DNA Repair (Amst)* 5:13–22.
15. Nardo T, et al. (2009) A UV-sensitive syndrome patient with a specific CSA mutation reveals separable roles for CSA in response to UV and oxidative DNA damage. *Proc Natl Acad Sci USA* 106:6209–6214.
16. Gorgels TG, et al. (2007) Retinal degeneration and ionizing radiation hypersensitivity in a mouse model for Cockayne syndrome. *Mol Cell Biol* 27:1433–1441.
17. de Waard H, et al. (2004) Different effects of CSA and CSB deficiency on sensitivity to oxidative DNA damage. *Mol Cell Biol* 24:7941–7948.
18. Licht CL, Stevensner T, Bohr VA (2003) Cockayne syndrome group B cellular and biochemical functions. *Am J Hum Genet* 73:1217–1239.
19. Fusteri M, Vermeulen W, van Zeeland AA, Mullenders LH (2006) Cockayne syndrome A and B proteins differentially regulate recruitment of chromatin remodeling and repair factors to stalled RNA polymerase II in vivo. *Mol Cell* 23:471–482.
20. Groisman R, et al. (2003) The ubiquitin ligase activity in the DDB2 and CSA complexes is differentially regulated by the COP9 signalosome in response to DNA damage. *Cell* 113:357–367.
21. Sveistrup JQ (2003) Rescue of arrested RNA polymerase II complexes. *J Cell Sci* 116:447–451.
22. Kamenisch Y, et al. (2010) Proteins of nucleotide and base excision repair pathways interact in mitochondria to protect from loss of subcutaneous fat, a hallmark of aging. *J Exp Med* 207:379–390.
23. Filippi S, et al. (2008) CSB protein is (a direct target of HIF-1 and) a critical mediator of the hypoxic response. *EMBO J* 27:2545–2556.
24. D'Errico M, et al. (2007) The role of CSA in the response to oxidative DNA damage in human cells. *Oncogene* 26:4336–4343.
25. Laposa RR, Feeney L, Crowley E, de Feraudy S, Cleaver JE (2007) p53 suppression overwhelms DNA polymerase eta deficiency in determining the cellular UV DNA damage response. *DNA Repair (Amst)* 6:1794–1804.
26. Herrup K, Neve R, Ackerman SL, Copani A (2004) Divide and die: Cell cycle events as triggers of nerve cell death. *J Neurosci* 24:9232–9239.
27. Diderich K, Alanazi M, Hoeijmakers JH (2011) Premature aging and cancer in nucleotide excision repair-disorders. *DNA Repair (Amst)* 10:772–780.
28. Kyng KJ, et al. (2003) The transcriptional response after oxidative stress is defective in Cockayne syndrome group B cells. *Oncogene* 22:1135–1149.
29. Murai M, et al. (2001) Early postnatal ataxia and abnormal cerebellar development in mice lacking Xeroderma pigmentosum Group A and Cockayne syndrome Group B DNA repair genes. *Proc Natl Acad Sci USA* 98:13379–13384.
30. Wijnhoven SW, Hoogervorst EM, de Waard H, van der Horst GT, van Steeg H (2007) Tissue specific mutagenic and carcinogenic responses in NER defective mouse models. *Mutat Res* 614:77–94.
31. Mangiarini L, et al. (1996) Exon 1 of the HD gene with an expanded CAG repeat is sufficient to cause a progressive neurological phenotype in transgenic mice. *Cell* 87:493–506.
32. Lawrence NJ, Sacco JJ, Brownstein DG, Gillingwater TH, Melton DW (2008) A neurological phenotype in mice with DNA repair gene *Erc1* deficiency. *DNA Repair (Amst)* 7:281–291.
33. Andressoo J-O, et al. (2006) An Xpd mouse model for the combined xeroderma pigmentosum/Cockayne syndrome exhibiting both cancer predisposition and segmental progeria. *Cancer Cell* 10:121–132.
34. Kraemer KH, et al. (2007) Xeroderma pigmentosum, trichothiodystrophy and Cockayne syndrome: A complex genotype-phenotype relationship. *Neuroscience* 145:1388–1396.
35. Vermeulen W, et al. (2001) A temperature-sensitive disorder in basal transcription and DNA repair in humans. *Nat Genet* 27:299–303.
36. Liang C, et al. (2006) Structural and molecular hair abnormalities in trichothiodystrophy. *J Invest Dermatol* 126:2210–2216.
37. Compe E, et al. (2007) Hypomyelination in trichothiodystrophy reveals the coactivator function of TFIIF. *Nat Neurosci* 10:1414–1422.
38. Borger DR, DeCaprio JA (2006) Targeting of p300/CREB binding protein coactivators by simian virus 40 is mediated through p53. *J Virol* 80:4292–4303.
39. Wallace DC (2005) A mitochondrial paradigm of metabolic and degenerative diseases, aging, and cancer: A dawn for evolutionary medicine. *Annu Rev Genet* 39:359–407.
40. Revet I, et al. (2011) Functional relevance of the histone gammaH2Ax in the response to DNA damaging agents. *Proc Natl Acad Sci USA* 108:8663–8667.
41. Mallery DL, et al. (1998) Molecular analysis of mutations in the CSB (ERCC6) gene in patients with Cockayne syndrome. *Am J Hum Genet* 62:77–85.
42. van der Pluijm I, et al. (2007) Impaired genome maintenance suppresses the growth hormone—insulin-like growth factor 1 axis in mice with Cockayne syndrome. *PLoS Biol* 5:e2.
43. Laugel V, et al. (2008) Deletion of 5' sequences of the CSB gene provides insight into the pathophysiology of Cockayne syndrome. *Eur J Hum Genet* 16:320–327.
44. Colella S, Nardo T, Botta E, Lehmann AR, Stefanini M (2000) Identical mutations in the CSB gene associated with either Cockayne syndrome or the DeSanctis-cacchione variant of xeroderma pigmentosum. *Hum Mol Genet* 9:1171–1175.
45. Horibata K, et al. (2004) Complete absence of Cockayne syndrome group B gene product gives rise to UV-sensitive syndrome but not Cockayne syndrome. *Proc Natl Acad Sci USA* 101:15410–15415.
46. Gorodetsky E, Calkins S, Ahn J, Brooks PJ (2007) ATM, the Mre11/Rad50/Nbs1 complex, and topoisomerase I are concentrated in the nucleus of Purkinje neurons in the juvenile human brain. *DNA Repair (Amst)* 6:1698–1707.
47. Ito S, et al. (2007) XPG stabilizes TFIIF, allowing transactivation of nuclear receptors: Implications for Cockayne syndrome in XP-G/CS patients. *Mol Cell* 26:231–243.
48. Jaarsma D, et al. (2011) Age-related neuronal degeneration: Complementary roles of nucleotide excision repair and transcription-coupled repair in preventing neuropathology. *PLoS Genet* 7:e1002405.
49. Newman JC, Bailey AD, Weiner AM (2006) Cockayne syndrome group B protein (CSB) plays a general role in chromatin maintenance and remodeling. *Proc Natl Acad Sci USA* 103:9613–9618.
50. Ljungman M, Zhang F (1996) Blockage of RNA polymerase as a possible trigger for u.v. light-induced apoptosis. *Oncogene* 13:823–831.
51. Proietti De Santis L, et al. (2002) Transcription coupled repair efficiency determines the cell cycle progression and apoptosis after UV exposure in hamster cells. *DNA Repair (Amst)* 1:209–223.
52. van der Horst GT, et al. (1997) Defective transcription-coupled repair in Cockayne syndrome B mice is associated with skin cancer predisposition. *Cell* 89:425–435.
53. Sands AT, Abuin A, Sanchez A, Conti CJ, Bradley A (1995) High susceptibility to ultraviolet-induced carcinogenesis in mice lacking XPC. *Nature* 377:162–165.